

LOW EMITTANCE 500 KV THERMIONIC ELECTRON GUN

K. Togawa*, T. Shintake, H. Baba, T. Inagaki, K. Onoe, T. Tanaka, SPring-8 / RIKEN Harima
Institute, Hyogo 679-5148, Japan

H. Matsumoto, High Energy Accelerator Research Organization (KEK), Ibaraki 305-5148, Japan

Abstract

A low emittance 500 kV thermionic gun has been developed for the injector system of the X-ray FEL project at SPring-8. A single-crystal CeB₆ cathode is chosen as a thermionic emitter, because of its excellent emission properties, i.e., high resistance against contamination, uniform emission density, and smooth surface. A gun voltage of -500 kV was chosen as a compromise between the need for suppressing emittance growth and reducing the risks of high voltage arcing. We have succeeded in producing a 500 keV beam with 1 A peak current and 3 μsec width. A normalized rms emittance of 1.1π mm.mrad has been measured by means of double-slit method. In this paper, we describe the design of the CeB₆ gun and report on the result of the emittance measurement.

INTRODUCTION

In X-ray FEL theory, it is well known that the fine structure of the beam dominates the FEL gain. To achieve the SASE-FEL in Angstrom wavelength region, the sliced emittance of the beam should be very low and the peak current should be of the order of kA. Moreover from the application point of view, the FEL machine should be stable for long periods of operation.

In the SASE-FEL, the electron beam generated by the gun is accelerated in the main linac, then it is directly injected into the long undulator and generates the X-ray beam there. Therefore, any electron bunch fluctuation in transverse position, timing, size, charge, etc., will directly affect the X-ray lasing. This is markedly different from the storage ring type machine situation. As a result, the stability of the electron gun is essential for producing stable X-ray FEL light.

We decided to use a thermionic cathode followed by a buncher system [1]. Basically, this is a traditional injector system used in many types of electron accelerators. High stability and long lifetimes have been routinely achieved in the present day injectors, however, for these conventional applications, the typical emittance is $\sim 30\pi$ mm.mrad or larger. In order to reduce the emittance, we have added the following modifications and upgrades:

1) Small size cathode. The initial emittance of the gun is dominated by its cathode size. We use a single crystal CeB₆ cathode with a 3 mm diameter. The theoretical thermal emittance is 0.4π mm.mrad at $\sim 1400^\circ\text{C}$. A high beam current of 3 A can be produced from the CeB₆ crystal at this temperature without jeopardising long lifetime.

2) Elimination of the cathode control grid. The

emittance of the traditional thermionic cathode gun is degraded by the electric field distortion caused by the grid mesh.

3) Applying 500 kV to the cathode. In order to minimize emittance growth due to space charge effects, a higher gun voltage is desirable. We use a 500 kV pulse just a few μsec in width.

4) Fast beam deflector. To form a nsec single bunch from the long pulse generated by the gun, we use a fast pulsed beam deflector after the gun.

5) Adiabatic bunching and acceleration. In order to minimize emittance growth due to the rf-field, a lower rf frequency is desirable. We use a 238 MHz sub-harmonic buncher, followed by a 1.6 m drift section, and then a 476 MHz booster cavity which raises the beam energy up to 1 MeV. A following S-band pre-linac is used to accelerate the bunch to 20 MeV before injection into the C-band main linac.

THE CEB6 GUN

We have designed and constructed a 500 kV electron gun with a CeB₆ cathode [2]. A side view of the CeB₆ gun with an emittance monitor bench is shown in Fig. 1, and the beam design parameters at the gun exit are summarized in Table 1.

Table 1 : The beam design parameters at the gun exit.

Beam energy	500 keV
Peak current	3 A
Pulse width (FWHM)	1.6 μsec
Repetition rate	60 Hz
Normalized emittance (rms)	0.4π mm.mrad

CeB₆ Cathode

The normalized rms thermal emittance of electrons emitted from a hot cathode is described by

$$\epsilon_{n,rms} = \frac{r_c}{2} \sqrt{\frac{k_B T}{m_e c^2}},$$

where r_c is the cathode radius, k_B is Boltzman's constant, and T is the cathode temperature. From the above relation, in order to obtain the small emittance less than 1π mm.mrad required for the X-ray FEL, the diameter of the cathode must be in the range of a few mm at the temperature of $1000-1500^\circ\text{C}$. On the other hand, very high emission density (~ 50 A/cm²) is required to produce a several ampere peak current from the small surface. Only the rare-earth hexaborides, such as LaB₆ or CeB₆ can emit such an intense current over long lifetimes. A single crystal is preferable for obtaining low emittance because of its extremely flat surface (roughness ≤ 1 μm)

* togawa@spring8.or.jp

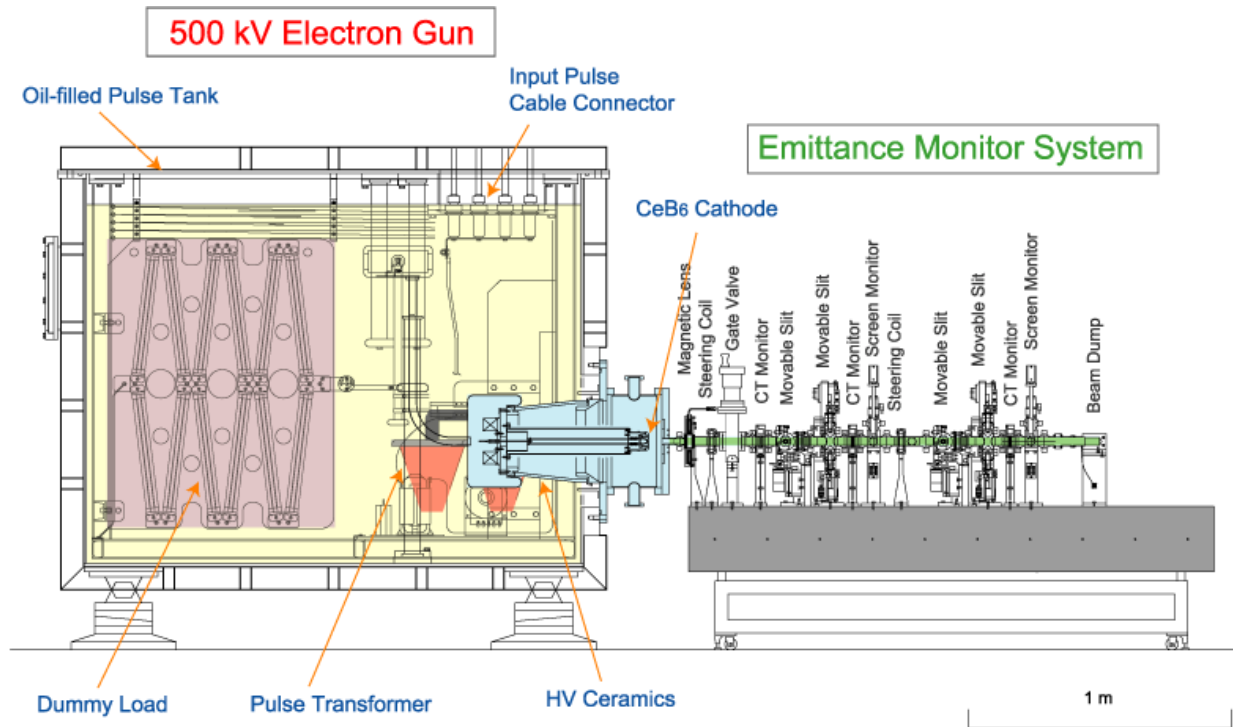


Figure 1: A side view of the CeB₆ electron gun with an emittance monitor bench.

with low porosity after surface material evaporation [3]. The emission density is more uniform because the crystal orientation is the same over the whole surface. In recent years, single crystal CeB₆ cathodes are widely used for electron microscope and superior stability has been demonstrated [4]. It is reported that CeB₆ is very resistant to carbon contamination as compared with LaB₆. Also the operational temperature of CeB₆ can be lower than that of LaB₆ because of its lower work function (~ 2.4 eV).

For the above reasons, we decided to use a single-crystal CeB₆ cathode with a [100] crystal face. The diameter of our CeB₆ cathode is 3 mm. 3 A peak current will be produced when heated to $\sim 1400^\circ\text{C}$. The theoretical thermal emittance is 0.4π mm mrad.

Fig. 2 shows the CeB₆ crystal, the cathode assembly and the cathode being heated in the test chamber. The CeB₆ crystal is mounted in a graphite sleeve. This produces a uniform electric field over the entire cathode surface. This is quite important for elimination of any beam emission halo coming from the cathode edge, which could cause damage to the undulator magnets.

We use a graphite heater rather than the conventional metallic filament made of tungsten or the like. Graphite is mechanically and chemically stable even at very high temperatures and does not evaporate like other metals. Since its electrical resistance does not change much

as a function of temperature, it is easy to control the heater power. The heater resistance is 0.18Ω .

A tantalum cylinder covers the graphite heater to shield the thermal radiation from its surface. A base plate for the cathode assembly is made of silicone nitride, which is mechanically strong even when thermal stresses are applied.

The cathode was heated up to $\sim 1400^\circ\text{C}$ in the test chamber by applying 210 W of heater power (see the

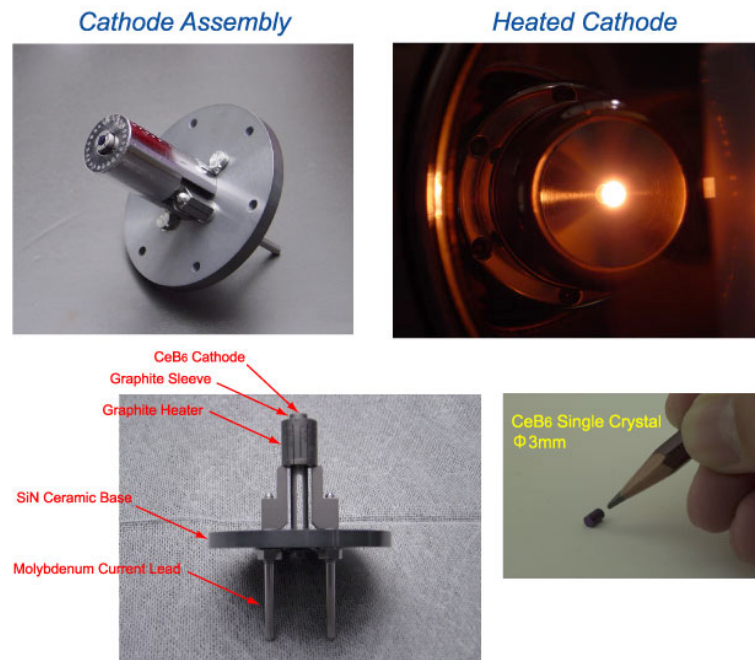


Figure 2: CeB₆ cathode assembly.

upper right side of Fig. 2). A reference temperature was measured from the graphite sleeve surrounding the cathode by means of a radiation monitor. We still need more study in order to determine the cathode temperature distribution precisely. Up to now, the cathode has been operated for 4000 hours without failure.

Accelerating Electrode

The accelerating electrode was carefully designed and manufactured because it controls the initial condition of the emerging low energy beam. We chose a flat Wehnelt rather than the common Pierce-type electrode. The reasons for this are as follows: (1) The Pierce electrode was originally designed to produce a parallel beam whose space charge field is balanced by a focusing electric field. However, if the cathode is not exactly centred due to misalignment of cathode mount or shifts in cathode position due to heating, an asymmetric focusing field acts on the beam. This may cause emittance growth. The flat Wehnelt does not have such an effect. (2) We planned to vary the beam current over a wide range in order to tune the accelerator system. The gun would be operated in a temperature limited region. The Pierce electrode is not suitable for such an operational mode, because at a low current, the beam is over-focused. The flat Wehnelt does not over-focus the beam.

Space charge limited current is described by

$$I_{scf} = \frac{4}{9} \epsilon_0 \sqrt{\frac{2e}{m_e}} \frac{S}{d^2} V^{3/2} \cdot F,$$

where V is the gap voltage, d is the electrode gap distance and S is the cathode area. In the case where the cathode radius is much smaller than d , the space charge limited current becomes higher than that of an infinite parallel electrode case of the equation's derivation. In order to take this effect into account, we introduce an enhancement factor, F into Child's law. By performing both an analytical evaluation and computer simulation using the EGUN code, it was found that the enhancement factor is a function of r_c/d . We set the gap distance d to be 50 mm. In this case, F becomes 4.5 and the space charge limited current is 10.5 A. Since this is much higher than the required current, the cathode will be operating in the temperature limited region. In that case, the electric field near the cathode surface is higher than it would be in the space charge limited region. Since the beam near the cathode is immediately accelerated, it is expected that emittance

degradation due to space charge effects would be minimized.

We performed a computer simulation for 500 keV, 3A beam operation using the EGUN code. As shown in Fig. 3, the beam trajectory does not diverge much by the electrode gap. When the calculation mesh size is set very fine, the phase space plot becomes a straight line, and the emittance without initial thermal motion converges to less than 0.1π mm.mrad for mesh sizes below 0.05 mm.

The maximum field on the Wehnelt edge is calculated to be 26 MV/m at 500 kV using the POISSON code. The electrode is carefully manufactured to avoid breakdown discharge problems at this high field. Ultra-clean stainless steel is used for the electrode material. The surface was chemically etched and rinsed with ultra-pure water to remove any hydrocarbon contamination which promotes discharges.

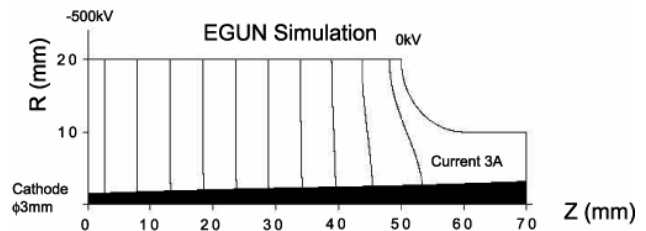


Figure 3: Beam trajectory near the gun electrode.

High-voltage Tank

The circuit diagram for the high-voltage tank is shown in Fig. 4. Basically, it follows the design conventional for a klystron tank. Nowadays, it is technically feasible to produce 500 kV pulses in high power devices, such as X-band klystrons. Therefore, we are able to use the same model C-band klystron modulator [5] to also feed a -24 kV pulsed voltage to the gun high-voltage tank. The

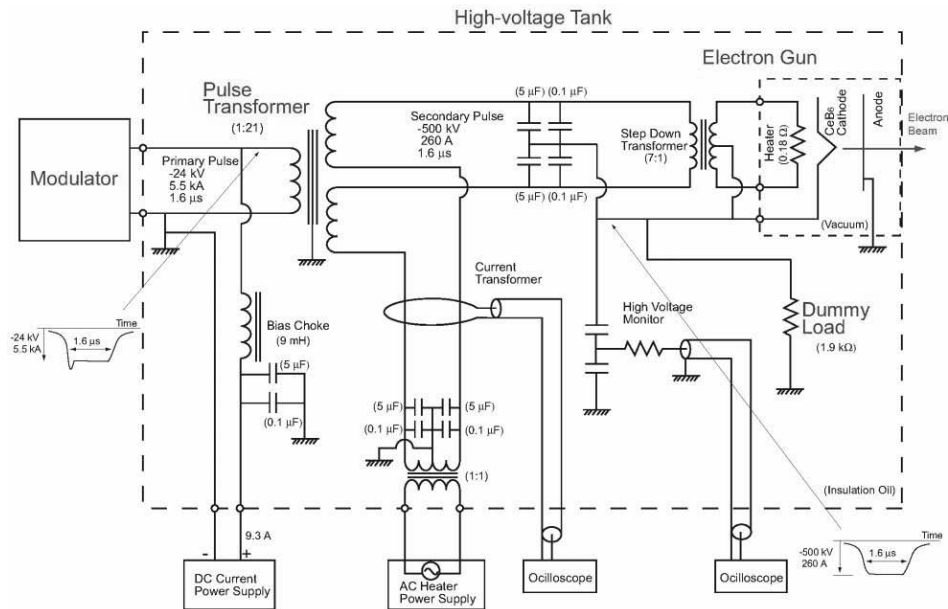


Figure 4: Circuit diagram of the gun high-voltage tank.

primary pulse is stepped-up to a -500 kV by a pulse transformer, with a turn's ratio of 1:21. In order to match the impedance of the gun to the modulator PFN output circuit, a 1.9 kΩ dummy load is connected in parallel with the cathode. AC power for the cathode heater is fed through the secondary winding of the pulse transformer. Since the heater current is very high (>30 A), a step-down transformer, whose turn's ratio is 7:1, is used to reduce the IR power loss in the transmission line from the power supply to the cathode.

Since we need to apply a -500 kV pulse voltage to the cathode, all the high-voltage components, namely, the ceramic insulator, pulse transformer, dummy load, etc., are immersed in insulating oil to eliminate discharge problems. Before operation, the high-voltage tank is pumped out to eliminate gases remaining in the oil and the high-voltage components.

Fig. 5 shows the waveform of the gun voltage and beam current. The beam current was measured by a current transformer (CT) located in the beam line right after the gun. The beam energy is 500 keV, and the peak current is 1 A. The flat-top portion of the pulse is about 0.8 μsec, which is sufficient to generate a nsec bunch.

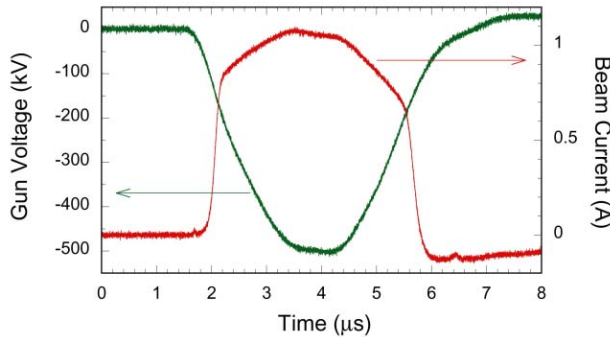


Figure 5: Waveform of the gun voltage and beam current.

EMITTANCE MEASUREMENT

We measured the beam emittance by the so-called double-slits method (Fig. 6). The upstream slit cut out a sheet shaped beamlet from the round beam, which spreads after passing through the drift space due to transverse thermal motion and space charge. The downstream slit measures the beamlet profile. By scanning the both slits throughout the whole beam area, the intensity profile in the phase space can be obtained.

We prepared four slits, two for horizontal (x-direction) scan and two for vertical (y-direction) scan. The upstream x-slit are located at 50 cm downstream from the cathode, followed by a 60 cm drift space and the downstream slit. The opening width must be narrow enough to ignore the beamlet broadening due to space charge. Fig. 7 shows the beamlet intensity profiles for several upstream slit width (25, 50, 100, 200 μm). The original beam energy and current was 400 keV and 0.9 A, respectively. The downstream slit width was set

to 25 μm. Accuracy of the width and position is better than 10 μm. The profile became Gaussian for the narrow width less than 100 μm, as expected from the thermal spread. The beamlet broadening due to space charge is ~15% of the thermal spread at 50 μm width in the experimental condition.

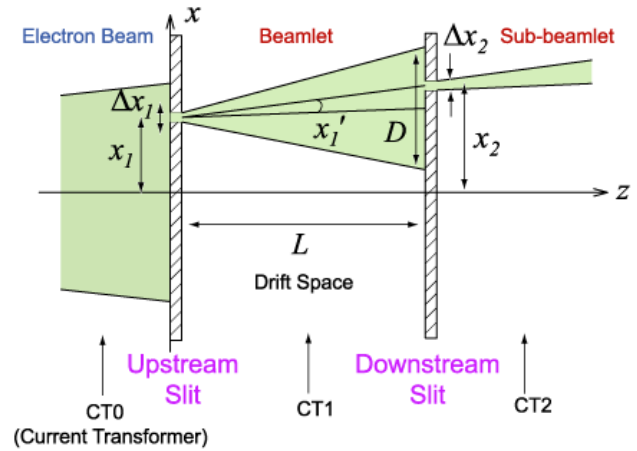


Figure 6: Principle of emittance measurement.

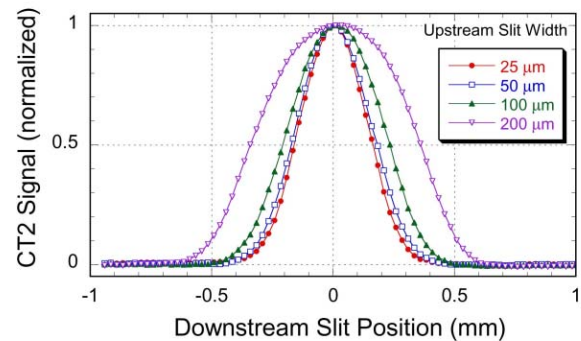


Figure 7: Beamlet profiles for different upstream slit width.

We found that the combination of a slit and a CT monitor with a digital scope is a very powerful tool to analyse the beam dynamics in time domain. The sub-beamlet current waveform provides the information about the time evolution of the phase space intensity at a certain point. From about 1500 waveforms stored by the slit scan, the time evolution of the phase space profile can be reconstructed. Fig. 8 shows an example of the animation screens of the phase space profile evolution.

Using a pair of vertical and horizontal slits, a time-resolved beam profile can be also measured by the same method.

We have measured the current density profile for the 500 keV beam with 1.0 A peak current. Fig. 9 shows the

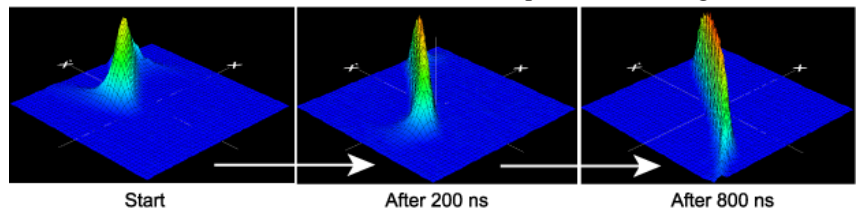


Figure 8: Time evolution of the phase space profile.

3-dimensional plot of the current density profile. The width for both the x- and y-slits was set to 0.5 mm × 0.5 mm and the scan step was 0.5 mm. It shows fairly flattop shape as we expected from the cathode geometry.

Fig. 10 shows the 2-dimensional plot of the phase space profile (x-direction) measured for the same beam parameters. The width for both the upstream and downstream slits was set to 50 μm and the scan step was 0.25 mm for the upstream slit and 0.1 mm for the downstream slit. From the phase space profile, we analysed the normalized rms emittance, defined as

$$\epsilon_{n,rms} = \beta\gamma\sqrt{\langle x^2 \rangle \langle x'^2 \rangle - \langle xx' \rangle^2},$$

where $\langle x^2 \rangle$, $\langle x'^2 \rangle$ and $\langle xx' \rangle$ denote mean square values weighted by current. The result was 1.1π mm mrad. The demonstrated beam parameter at gun exit are summarized in Table 2.

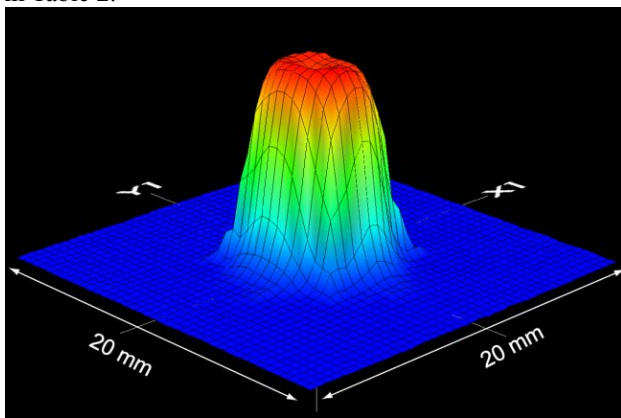


Figure 9: Current density profile of the 500 keV, 1.0 A beam.

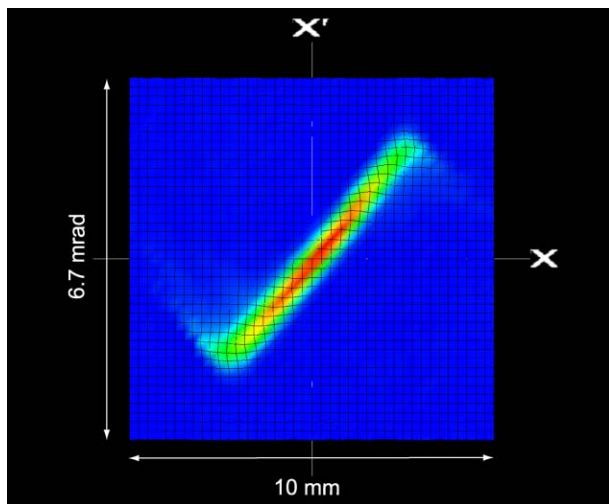


Figure 10: Phase space profile of the 500 keV, 1.0 A beam.

Table 2: Demonstrated beam parameters at gun exit.

Beam energy	500 keV
Peak current	1 A
Pulse width (FWHM)	3 μsec
Repetition rate	10 Hz
Normalized emittance (rms)	1.1π mm.mrad

IMPROVEMENTS FOR X-RAY FEL

Based on the experimental results, the following improvements will be done for the real injector system:

1) Beam current: We need to increase the beam current by a factor of 3 for operation. The current cathode emission may not be activated well as possible. The increase in cathode temperature to obtain a 3 A peak current is estimated to be ~120°C.

2) Pulse width: The high-voltage pulse width turned out to be two times longer than the design value. The fairly big stray capacitance of the dummy load resistors no doubt causes the pulse to be stretched out to this long duration. As a result, the heat load that must be removed from the high-voltage tank was higher than the design expectation. The large size of the high-voltage tank is also determined by the resistors. In order to shorten the pulse width and to make the tank more compact, we are now developing an electron tube dummy load, which will replace the load resistors.

3) Emittance: We successfully achieved a very small emittance, but even so, it was somewhat larger than the theoretical predicted value. A small tail at the profile edge, which may be generated by the space charge effect, is a source of the emittance increase. The emittance without this tail can be roughly estimated by making the product of the rms diverging angle at the beam centre (σ_x) and the rms beam radius ($\sim r/2$). The 0.6π mm.mrad value obtained is near the theoretical thermal emittance. Since the nonlinear tail comes from the edge region of the round beam, it could be removed by using a beam collimator. We expect that doing that we should realize the required small emittance of less than 1π mm.mrad.

REFERENCES

- [1] T. Shintake et al., "SPRING-8 Compact SASE Source, SPIE2001, San Diego, USA, June 2001
- [2] K. Togawa et al., "CeB₆ Electron Gun for the Soft X-ray FEL Project at SPRING-8", FEL2003, Tsukuba, Japan, Sept. 2003, Nucl. Instr. Meth. A 528 (2004) 312
- [3] H. Kobayashi et al., Emittance Measurement for High-Brightness Electron Guns, 1992 Linear Accelerator Conference, Ottawa, Canada, August 1992
- [4] <http://www.feibeamtech.com/>
- [5] H. Matsumoto et al., "A Closed Compact Modulator for 50 MW C-band (5712 MHz) Klystron" 25th International Power Modulator Symposium and 2002 High Voltage Workshop, Hollywood, USA, 2002, ISBN 0-7803-7540-8
- [6] K. Togawa et al., "Emittance Measurement on the CeB₆ Electron Gun for the SPRING-8 Compact SASE Source FEL Project", APAC2004, Gyeongju, Korea, March 2004